Soft Matter

PAPER

View Article Online
View Journal | View Issue

Cite this: *Soft Matter*, 2016, 12, 4375

Compressing a spinodal surface at fixed area: bijels in a centrifuge

Katherine A. Rumble, Job H. J. Thijssen, Andrew B. Schofield and Paul S. Clegg*

Received 21st January 2016,
Accepted 4th April 2016

DOI: 10.1039/c6sm00168h

www.rsc.org/softmatter

Bicontinuous interfacially jammed emulsion gels (bijels) are solid-stabilised emulsions with two inter-penetrating continuous phases. Employing the method of centrifugal compression we find that macroscopically the bijel yields at relatively low angular acceleration. Both continuous phases escape from the top of the structure, making any compression immediately irreversible. Microscopically, the bijel becomes anisotropic with the domains aligned perpendicular to the compression direction which inhibits further liquid expulsion; this contrasts strongly with the sedimentation behaviour of colloidal gels. The original structure can, however, be preserved close to the top of the sample and thus the change to an anisotropic structure suggests internal yielding. Any air bubbles trapped in the bijel are found to aid compression by forming channels aligned parallel to the compression direction which provide a route for liquid to escape.

1 Introduction

Bicontinuous interfacially jammed emulsion gels, known as bijels, are a relatively new class of solid-stabilised emulsions with two inter-penetrating continuous phases and a large interface between them.[1,2] Their formation requires the arrest of the spinodal decomposition of a binary liquid mixture using neutrally wetting solid particles. These particles become irreversibly adsorbed onto the interface[3] and prevent further phase separation by jamming, thus forming a long-lived stable bicontinuous structure.[4] The mechanical strength of the structure can be attributed to this jamming of solid particles at the interface.[5] It is expected that yielding will occur in response to an expansion of the liquid interface and hence an unjamming of the particles.[2] Carefully controlled unjamming and re-jamming could lead to training of the structure.

The bijel has many highly desirable properties such as the large surface area and the zero mean curvature of the interface. In addition, the pore size and distribution are within the experimentalists' control and the material has long-range connectivity which leads to efficient mass transport.[6] Potential applications include cross-flow microreactors and separation processors which utilise the long-range connectivity and the containment of two immiscible liquids within separate continuous flows within the bijel structure.[7] A step towards the utilisation of bijels has been made by Lee and Mohraz who have created a method to form bicontinuous structures from various materials using the bijel as a template to create a polymer scaffold.[8] Recently the bijel templating method has been utilised to create electrodes where the bicontinuous structure allows for the optimisation of the active surface area and mass transport.[9,10] Others have found ways to avoid precisely tuning the particle wettability.[11,12] Additionally, Haase *et al.* have developed a new technique to create bijel fibres and thin membranes using solvent transfer induced phase separation which simplifies fabrication and allows a larger range of templating liquids to be used.[13]

While the potential applications of the bijel are varied, with progress having been made towards implementation,[4,5,8–10,12–16] little work has considered the fundamental mechanical properties. Before any applications can be realised it is necessary to test whether the structure can withstand the stresses applied during necessary processing steps and the general use of the product. Furthermore, linking macroscopic properties with microscopic changes will allow for the tuning of the microscopic structure in order to obtain the optimum bijel.[17]

Previous experiments investigating the structural integrity of bijels have been largely qualitative. These have included both shear stress and compressive stress experiments. Shear experiments deform the sample at fixed volume whereas compression experiments either result in the expulsion of fluid or expansion in other directions. Firstly, upon dropping a small wire into a 2,6-lutidine–water bijel, Herzig *et al.* found that the wire sunk with decreasing velocity before entering a regime of intermittent falling and finally stopped indicating that the bijel exhibits both viscoelastic properties and a yield stress. It was hypothesised that this intermittent movement was due to the local rearrangement of particles on the interface caused by the stress of supporting the weight.[1] Secondly, the qualitative response of

School of Physics and Astronomy, James Clerk Maxwell Building, Peter Guthrie Tait Road, Edinburgh, UK EH9 3FD. E-mail: paul.clegg@ed.ac.uk

ethanediol–nitromethane bijels to compressional stress and shear stress has been investigated. These bijels were imaged before, during and after the experiments and thus it was observed that the connectivity of the particle network can change in response to shear with the domains orientated in the direction of the shear. In response to a localised perturbation the bijel was observed to resume its original state after the removal of the compressional stress indicating that the bijel displays elastic behaviour.[4] More recent research has also investigated the rheological properties of bijels of both liquid pairs using oscillatory shear. These experiments have shown that the bijel can indeed be described as a gel since the elastic behaviour becomes more prominent than the viscous behaviour upon formation.[6]

Here we employ the method of centrifugal compression combined with confocal microscopy in order to investigate the macroscopic and microscopic changes to the bijel induced by a well-controlled compressional force. Due to the preferential wetting of the vial by one of the solvents the bijel structure appears to slide freely and hence experiences pure compression. This force is given by

$$F = m\omega^2 r \quad (1)$$

where r is the radius from the axis of rotation, m is the mass of the sample above r and ω is the angular velocity. This method has previously been used to probe the mechanical properties of a dispersion of incompressible polymer beads and droplet emulsions stabilised by hard sphere particles.[18–20] For the polymer beads, a maximum strain was observed due to the incompressible nature of the particles.[18] For the emulsions, it was found that faster angular velocities led to compression to higher volume fractions of droplets and that towards the bottom of the sample the droplets become more deformed due to an increased compressive force at this location (see eqn (1)). In addition, the solid stabilised structure was observed to change shape under centrifugal compression.[19] This training of the structure has also been observed in simulations of phase separating systems, such as the bijel, when phase separation was performed under electric or magnetic fields.[21,22] All four of the above effects are expected to be observed in the compression of the bijel.

Firstly, in this article the macroscopic changes in the final height of the sample and how these are linked to the initial permeability and the domain size of the bijel will be discussed. Secondly, confocal microscopy images will be used to analyse the changes in the microstructure of the bijel. This will be done using a Fourier transform method to extract quantitative information about the deformations in the structure. Finally, the behaviour of trapped air bubbles within the bijel and the effect they have on compression *via* the permeability will be described.

2 Experimental section

2.1 Materials

Ethanediol (anhydrous, 99.8%) and hexamethyl disilazane (HMDS) (reagent grade, ≥99%) were purchased from Sigma-Aldrich. Nitromethane (≥99%, for analysis) was purchased from Acros Organics and stored under nitrogen gas. Ammonia (35%, Certified AR for analysis) was purchased from Fisher Scientific, fluorescein was purchased from BDH and absolute ethanol (AnalaR NORMAPUR) was purchased from VWR; all chemicals were used as received. The silica particles were made *via* the Stöber method[23] and rhodamine B isothiocyanate (RITC), purchased from Fluka, was used to fluorescently label the particles. The particle radius was determined by SEM to be 0.29 ± 0.02 μm.

2.2 Methods

The surface of the rhodamine B doped silica particles was modified with hexamethyldisilazane (HMDS) to obtain neutral wetting. Relevant concentrations of HMDS were added to a 2.4 wt% solution of rhodamine B doped particles in ethanol followed by 0.7 g of ammonia solution (35%). The mixture was stirred at 1000 rpm for 24 hours at room temperature before the particles were washed with ethanol five times. The particles were then dried in an oven at 110 °C for half an hour to evaporate the solvent before drying for a further hour under full vacuum. In between these steps the particle 'cake' was ground up: a key step to achieving the correct wetting properties. Once dried the particles were used immediately.

Bijels were formed by first measuring out the desired volume fraction of the HMDS modified rhodamine B doped particles, followed by nitromethane and then the fluorescein doped ethanediol. It is essential to ensure that the critical composition (64 : 36 mass fraction nitromethane : ethanediol) is maintained by adding the correct mass of ethanediol to the mass of nitromethane actually added. This mixture was then heated and the particles were simultaneously dispersed in a hot ultrasonic bath. The hot mixture was transferred into a preheated (56 °C) glass cuvette with a 1 mm pathlength before this was quenched to room temperature using a stirred water bath. The samples were then observed using a Zeiss LSM 700 laser scanning microscope, with the 555 nm and 488 nm laser lines being used for excitation of rhodamine B and fluorescein, respectively, to determine if a bijel has indeed been formed. Filters were used as appropriate.

The centrifugal compression experiments were carried out by placing the cuvette containing the bijel sample in a protective silicone cover into the thermostated Thermo Scientific 3SR Plus Multifuge centrifuge for 5 minutes at various rotation speeds at room temperature (see Fig. 1a). The internal structure of the samples was observed after centrifugal compression again on the Zeiss laser scanning confocal microscope. The height measurements of the bijel were taken using a mounted calliper accurate to 0.1 mm. The bijel domain sizes are determined using a pixel counting algorithm in MATLAB (Mathworks) which evaluates the product of brightness intensities between pixels of given distances apart from the fluorescein labelled ethanediol image and then takes an average across the whole image. The distance between pixels where the first minimum in the product of brightness intensities occurs then represents the interfacial separation.

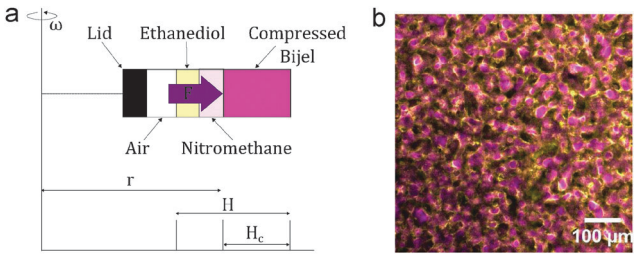

Fig. 1 (a) Schematic of the experimental set-up for centrifuging bijels. (b) A confocal microscopy image of the initial structure of a typical bijel with 5 vol% particles and an interface separation of 27 μm. The ethanediol phase is coloured magenta and the particles are coloured yellow.

3 Results and discussion

The bijels used in this work consisted of continuous ethanediol-rich and nitromethane-rich domains separated by a layer of silica particles at 4 vol%, 5 vol% or 7 vol% (see Fig. 1b). These structures are stable and were not observed to collapse for more than 100 hours under terrestrial gravitational conditions.

3.1 Macroscopic

We observe that when the bijel is compressed in a centrifuge nitromethane and ethanediol are resolved into two layers on top of the compressed bijel structure (see Fig. 2a). At high angular acceleration (360*g*) almost complete destruction of the structure is observed with the two liquids fully resolved above a particle fraction. The latter has a volume fraction that is approximately 3 times the initial volume fraction of particles. Here, a highly compressed structure remains which contains a large fraction of particles and a small fraction of the liquids (see Fig. 2a). At lower angular accelerations the bijel structure still significantly decreases in height but is not completely destroyed; the height achieved (H_c) depends on both the angular acceleration and the centrifugation time. Here we focus on low angular accelerations (14–27*g*) and short times (increments of 5 minutes).

The changes in height (or height ratio (H_c/H)) of the bijel structure with the centrifugation time at a constant angular acceleration (14*g*) have been investigated (see Fig. 2b). Fig. 2b shows that at short times the change in height is substantial however this change decreases and approaches a plateau after approximately 30 minutes. As the particle volume fraction decreases the final height ratio achieved by the sample decreases. The shape of the curve also changes with particle volume fraction and for samples with larger particle volume fraction a much more gradual variation from the initial rapid compression to the plateau is observed. This implies that the particle volume fraction and thus the domain size play an important role in the stability of the bijel. This could be due to either the increase in the amount of elastic interface or the lower permeability of the fluid domains, or both.

The permeability of the structure describes the ease with which liquid moves through the porous medium and can be calculated from the graphs of sample height *versus* time.[24]

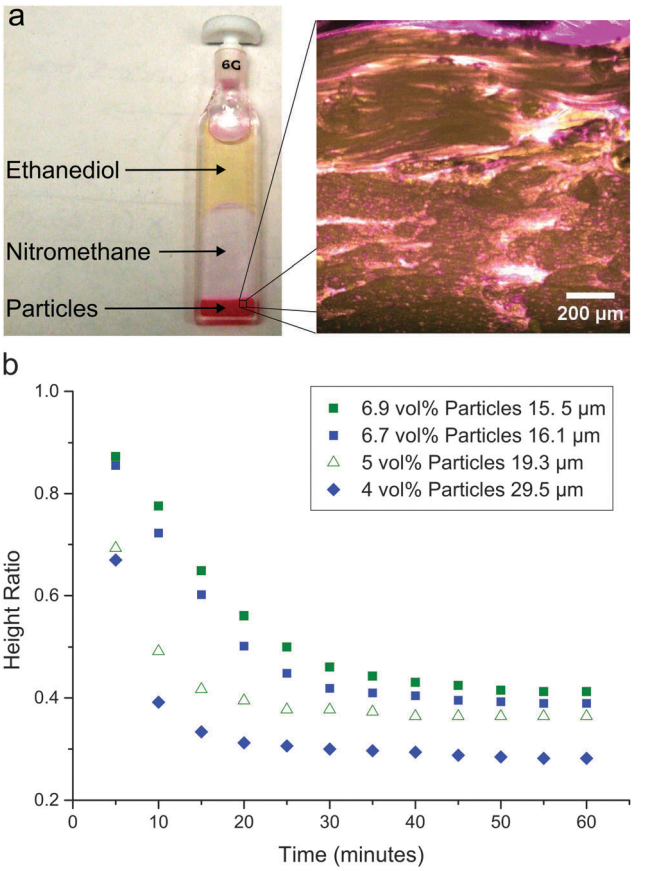

Fig. 2 (a) An image showing the appearance of a bijel with 3 vol% particles and an interface separation of 60 μm that has been completely destroyed by centrifugal compression at 360*g* for 30 minutes. A confocal image of the structure of the particle fraction is also shown where the particles are coloured yellow and the ethanediol coloured magenta. (b) A height ratio (H_c/H) *versus* time graph for samples made with 7 vol% (filled squares), 5 vol% (open triangles) and 4 vol% (filled diamonds) of particles with different domain sizes centrifuged at 14*g*.

We take the permeability to be

$$k_0 = \frac{-a^2}{(1-\phi_0)u_0}\left.\frac{\mathrm{d}h}{\mathrm{d}t}\right|_0 \qquad (2)$$

where a is the particle radius, ϕ_0 is the particle volume fraction, $\left.\frac{\mathrm{d}h}{\mathrm{d}t}\right|_0$ is the initial slope of the height *versus* time graph in units of ms^{-1} and u_0 is the sedimentation rate of an isolated particle. The latter quantity is calculated using

$$u_0 = \frac{2a^2\Delta\rho g}{9\eta_s} \qquad (3)$$

where $\Delta\rho$ is the difference in density between the solid particles and the liquid with the lowest density, g is the centrifugal acceleration and η_s is the background solvent viscosity which is estimated by combining the viscosities of nitromethane and ethanediol in terms of the ratio 64 : 36.[24] This approach is based on the theory of sedimenting gels proposed by Buscall and White which considers the balance of the viscous drag

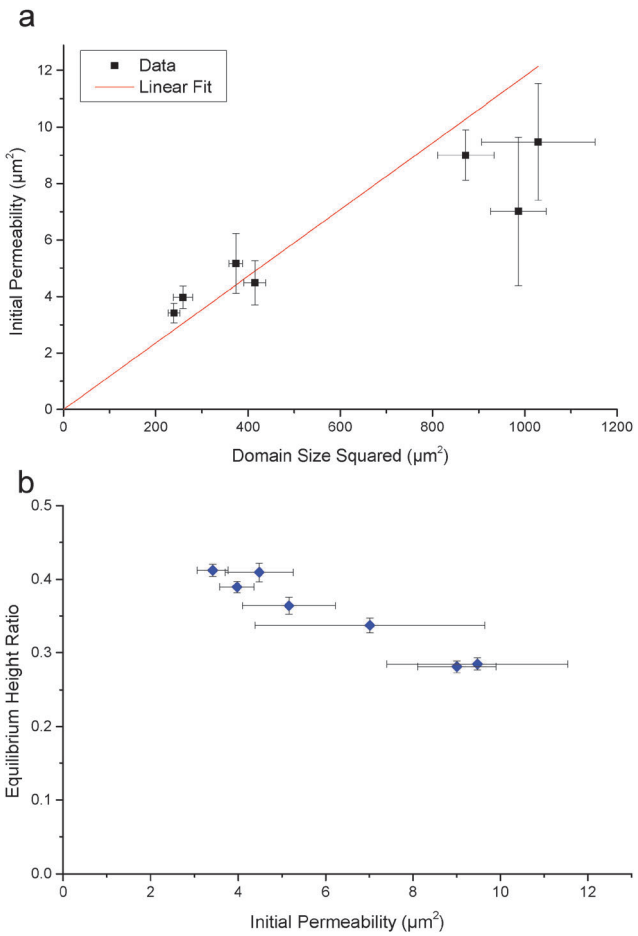

Fig. 3 (a) A graph showing the relationship between the initial permeability and the square of the domain size of samples centrifuged at 14*g*. (b) A graph showing the relationship between the initial permeability and the final height ratio achieved after 1 hour of centrifugation at 14*g*.

force, the gravitational force and network stress to give the rate of change in sediment height with time.[25]

The initial permeability of the bijel, determined using eqn (2), can be used to establish whether the movement of liquids throughout the structure affects the compression process. Fig. 3a shows that the permeability is proportional to the square of the domain size which is consistent with many models of fluid flow through porous media.[26] This indicates that the ease with which the liquids can move through the bijel is irrevocably linked to the size of the internal structure of the bijel. This also agrees with the result of Huh *et al.* where the initial permeability was observed to scale with the pore area for sedimenting gels.[24] Secondly, the equilibrium height ratio, calculated as the compressed final height divided by the initial height (H_c/H), after one hour of centrifugation at 14*g* is plotted against the initial permeability in Fig. 3b. This shows that as the initial permeability increases the equilibrium height ratio decreases. This could indicate that the compression of the bijel is determined by the movement of the two liquids out of the bijel structure which in turn depends on the size of the internal domains of the bijel. Similarly, it has been observed by Manley *et al.* that the initial rate of gravitational collapse of colloidal gels is controlled by the movement of fluid out of the structure.[27] However, it is also possible that both the permeability and final compressed height could be controlled by the interface separation leading to the observed correlation between the two.

In principle, slight changes to sample temperature could occur within the centrifuge. This could potentially influence the sample response *via* changes to the interfacial tension. Preliminary studies, on the effect of five minutes of centrifugation at elevated temperature, showed no effect on the height ratio. We did not investigate this further here.

3.2 Microscopic

It is not just the macroscopic height of the bijel that changes under centrifugal compression, the internal structure of the bijel is also modified. In fact, an anisotropic bijel structure emerges as a result of this compression (see Fig. 4). In three dimensions this structure appears to be sheet-like with a large domain size in two directions and a very small domain size in the third direction which can be seen in the orthogonal projections in Fig. 4. These sheets are orientated with the flat surface perpendicular to the centrifuge arm and the small domains parallel to the centrifuge arm. This means that the domains have aligned perpendicular to the applied compressional force as has also been observed when compressing a bicontinuous polymer blend in a squeeze flow experiment.[28] In addition, the structure observed here appears to be similar to that achieved *via* spinodal decomposition close to a wall[29] and we note that the base of the cuvette could play an analogous role to the wall. Indeed, a wetting layer of ethanediol at the glass is observed surrounding the bijel including at the base

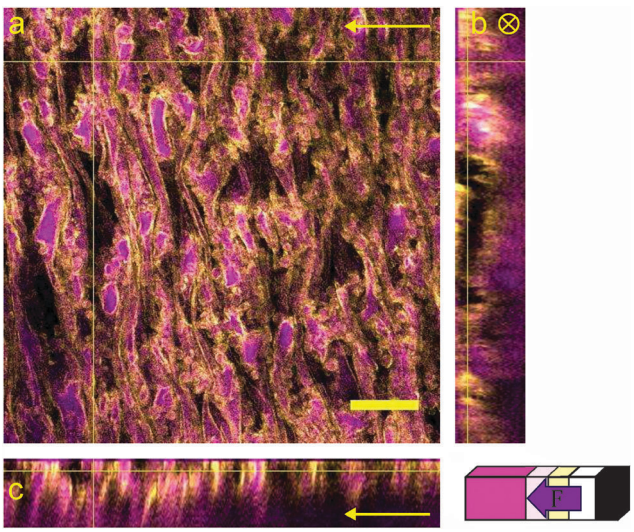

Fig. 4 Confocal microscopy image of a distorted compressed bijel including the orthogonal projections with 5 vol% particles and an interface separation of 29 μm and centrifuged at 20*g* for 10 minutes. The ethanediol rich phase is coloured magenta, the particles are coloured yellow and the arrows show the direction of compression. The scale bar is 50 μm. This image has been deconvoluted using the Huygens software (Scientific Volume Imaging).

both before and after centrifugation. The anisotropic compressed bijel structure (see Fig. 4) strongly suggests that negative feedback occurs: as compression progresses solvent withdrawal from the structure becomes more difficult. This is observed experimentally in the height *versus* centrifugation time graphs where as the time increases the rate of height decrease is reduced (see Fig. 2b). This is in complete contrast to the initial collapse of colloidal gels where a positive feedback loop is observed; as collapse occurs channels open up and the solvent flow is increased.[30]

It has also been observed that (1) the anisotropic structure, once formed, is permanent and (2) that the height of the compressed sample does not recover; a phenomenon which was also observed for some emulsions centrifuged by Maurice *et al.*[19] After centrifugal compression, observations for 3870 minutes show that there is no elastic recovery of the height of the sample. One reason for this is that the liquids cannot easily return to the right domains. This is due to the domains of the ethanediol becoming closed off by particles since a nitromethane rich phase sits on top of the compressed structure (see Fig. 2a). Nonetheless, in principle, the internal anisotropy could relax at a fixed height, but does not, since the anisotropic structure is observed to be stable over time. This contrasts with previous observations of a local perturbation which was only applied for a few seconds and then removed with no macroscopic ejection of liquids.[4] Our results mean that the distorted interfaces must themselves be jammed. In addition, Fig. 5a shows that at the top of the compressed sample the structure can remain isotropic whilst at the bottom the structure is anisotropic. These structures remain intact and hence the structures of both regions must be locally jammed. These observations support the idea that the yielding is an unjamming and re-jamming process.[1] The particles are the heaviest component in the system and thus under centrifugation they move in the direction of the centrifugal force. Since the particles are essentially irreversibly adsorbed to the interface, the interface between the liquids is then dragged along with the particles leading to an increase in the total interfacial area and hence an unjamming of the particles. Then, when the stress is removed, the interface contracts driven by the interfacial tension and the particles are re-jammed in their new positions creating these structures.

As we have seen, the compressed anisotropic bijel structure (seen in Fig. 4) is not always observed throughout the whole of the compressed sample. In some samples centrifuged at low angular acceleration the top of the bijel appears to descend without changes to the internal structure in agreement with the model of Buscall and White.[25] However, the bijel becomes increasingly anisotropic approaching the bottom of the cuvette (see Fig. 5a). This effect has been quantified by analysing the fast Fourier transform (FFT) of the confocal microscopy images of the internal structure of the bijel at various distances from the cuvette base. A heuristic model which fitted the line shape (two Lorentzian fits summed together) was employed in order to analyse the peak in the FFT in the horizontal and vertical directions of the image (see the inset in Fig. 5b). From the fitted

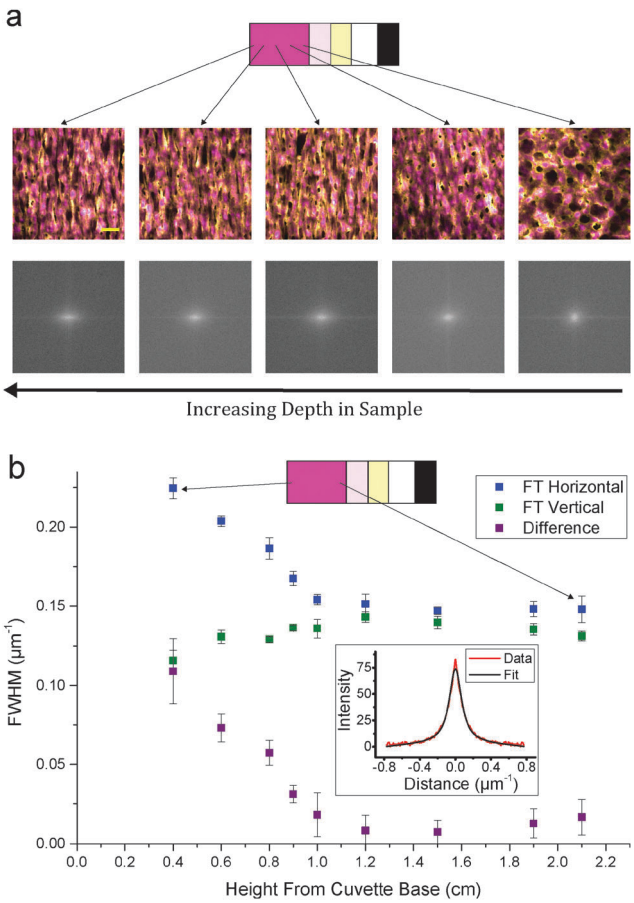

Fig. 5 (a) Images of a compressed bijel with 5 vol% particles and an interface separation of 32 μm which was centrifuged at 15*g* for 5 minutes with increasing depth in the sample where the ethanediol rich phase is coloured magenta and the particles are coloured yellow. The scale bar is 50 μm. The bottom line is the fast Fourier transform (FFT) of these images. (b) A graph showing the full width half maximum (FWHM) of the FFT peak obtained using a heuristic fit function *versus* the height from the cuvette base. The schematic shows the orientation within the sample. Inset: A graph showing a peak from the fast Fourier transform (red) and the respective fit functions (black).

line shape the full width half maximum (FWHM) of each peak was extracted and the values obtained for one sample are plotted in Fig. 5b. Initially, the FWHM in both the horizontal and vertical directions of the image are similar and remain constant. However, at a certain height from the base of the cuvette the FWHM in the horizontal direction increases rapidly and the FWHM in the vertical direction decreases slightly. This change can be associated with the transition from the initial isotropic bijel to that of the anisotropic bijel structure. The degree of anisotropy of the structure appears to increase from this point indicating that the structure becomes more compressed towards the base of the cuvette. This can be attributed to the increase in the radius from the axis of rotation and the increase in the mass above the sample both leading to an increase in the compressional force experienced by the sample (see eqn (1)). At some height the yield stress of the structure appears to be exceeded.

The FWHM data which were taken from samples after five minutes of centrifugation can be represented in the form of a

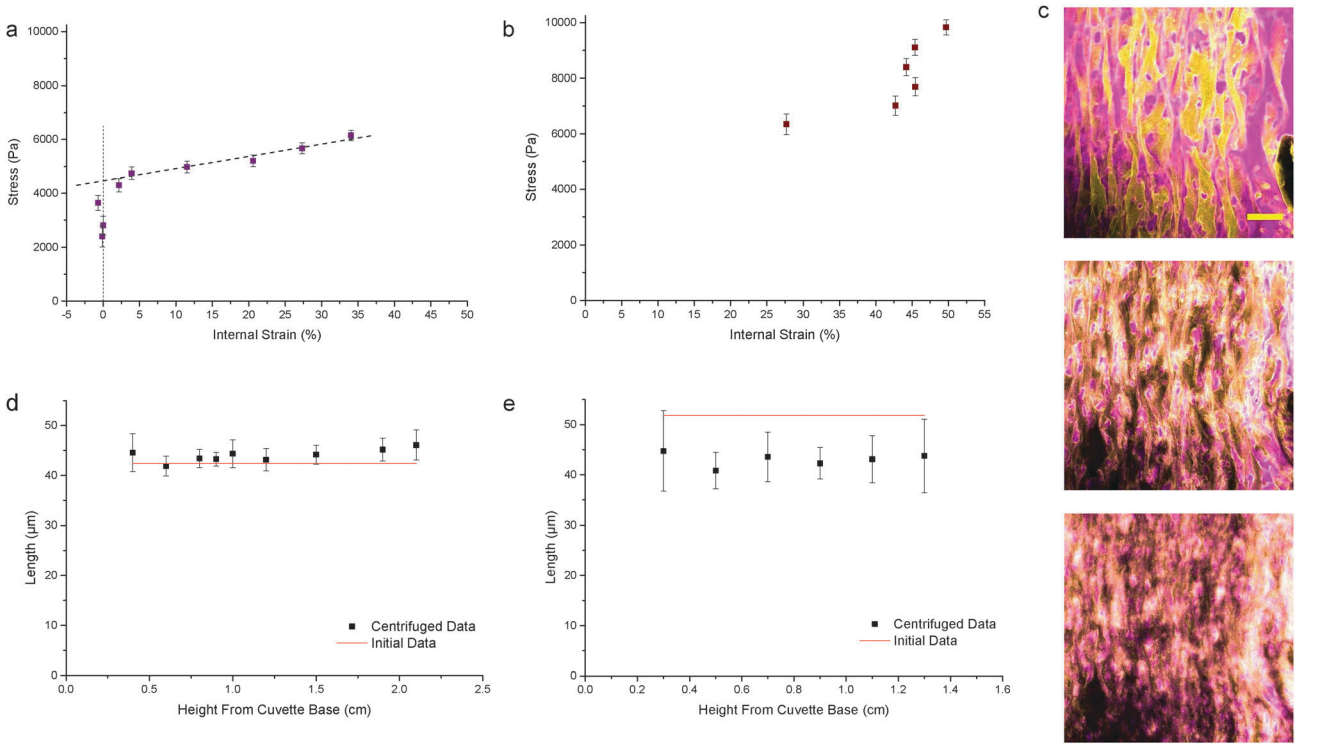

Fig. 6 (a) A graph showing the stress *versus* internal strain for a sample with 5 vol% particles after centrifugation at 16.6*g* for 5 minutes. (b) A graph showing the stress *versus* internal strain for a sample with 5 vol% particles after centrifugation at 24.8*g* for 5 minutes. (c) Three confocal images in a *Z*-stack at the location of a kink from a bijel with 5 vol% particles and an interface separation of 27 μm which was centrifuged at 20*g* for 5 minutes. The top slice is at the glass wall and the next two slices are further into the sample. The scale bar is 50 μm. (d) The length of a side of a cube calculated from the FWHM data assuming the unchanged surface area for the same sample as shown in (a) with the distance from the cuvette base. (e) The length of a side of a cube calculated from the FWHM data assuming the unchanged surface area for the same sample as shown in (b) with the distance from the cuvette base.

stress *versus* internal strain graph (see Fig. 6a and b). The stress can be calculated from the force (see eqn (1)) at the different locations within the cuvette divided by the area. We define the internal strain to be the deformation of the internal structure of the bijel. We quantify this by the anisotropy of the liquid domains and we then assume that this is linearly proportional to the compressive strain. The anisotropy is calculated from the relationship between the FWHM in the horizontal direction of the image in the compressed sample and that of the sample before compression. This then quantifies the deformation of the internal structure of the bijel compared to the structure before centrifugation. We calculate the strain, ε, from a compression experiment using

$$\varepsilon = \frac{a_0 - a}{a_0} \tag{4}$$

where a_0 is the initial length scale and a is the compressed length scale. Here, the deformations of the bijel are quantified in Fourier space and thus we have to consider $q_0 = \frac{2\pi}{a_0}$ and $q = \frac{2\pi}{a}$ where q_0 and q are the initial and compressed length scales in Fourier space. Using the extracted FWHM we find that the internal strain is

$$\varepsilon_{\text{int}} = 1 - \frac{q_0}{q}. \tag{5}$$

Such a graph is shown in Fig. 6a for a sample centrifuged for five minutes at low angular acceleration (14–18*g*) and here the internal strain is initially constant and centred around zero. In this region of the sample the internal structure of the uncompressed bijel is maintained. However, at a certain stress the strain observed within the sample starts to increase. This suggests that the bijel structure exhibits internal yielding where the structure starts to become anisotropic (see Fig. 4). A yield stress has previously been hypothesised to be present for the bijel and thus this result is qualitatively consistent with previous findings.[1,4] Herzig *et al.* crudely estimated that for a 2,6-lutidene–water bijel stabilised by 2 vol% particles the lower bound of the bijel yield stress would be 600 Pa.[1] This is an order of magnitude lower than the approximate internal yield stress obtained here however the bijels used in this study contained different liquids (ethanediol–nitromethane) and were stabilised by a higher particle volume fraction (5 vol%) which would increase the yield stress.

At higher angular accelerations (19–27*g*) the samples display altogether different behaviour; the bijel initially already exhibits an internal strain but rather than smoothly increasing with the stress a kink appears (see Fig. 6b). The data do not display zero strain initially because the entire structure is deformed to a significant extent due to the larger compressional stress. The kink, where the internal strain remains constant or in fact decreases with increasing stress, is observed to be present in all samples centrifuged at higher angular acceleration. This kink

(or kinks in some cases) does not appear to be related to the presence of trapped air bubbles within the sample or the channels they form (see below). However, taking a closer look at the confocal microscopy images, large light and dark regions are observed in the vertical direction of the images. This would indicate that compression also occurs on a larger length scale with the entire structure buckling in places. This may then lead to a constant anisotropy being observed microscopically in the compressed bijel structure. We suggest that this occurs because there is a wetting layer of ethanediol surrounding the glass which the compressed sample can move laterally into. Indeed, in *Z*-stacks taken in the kink region it can be observed that the sample has begun to bulge towards the glass on a length scale of approximately 0.1 mm (see Fig. 6c). This indicates that it is necessary to consider more than one length scale when assessing the effect of compression on the bijel. Such behaviour is not, however, observed in samples centrifuged at lower angular accelerations.

The FWHM data in both the horizontal and vertical directions can be used to assess whether the surface area of the interface changes. This is done by modelling the initial domains as cubes with equal sides and the compressed domains as oblate cuboids with two long sides and one short side. The length l of the side of an equivalent cube with an equal surface area can be calculated from the reciprocal of the FWHM in the vertical ($v = 2\pi/\mathrm{FWHM}_v$) and the horizontal ($h = 2\pi/\mathrm{FWHM}_h$) directions:

$$l = \sqrt{\frac{v^2 + 2vh}{3}}. \quad (6)$$

The values for l after a compression experiment for the two samples shown in Fig. 6a and b are plotted against the height from the cuvette base in Fig. 6d and e, respectively. The value of l for the initial uncompressed structure is shown as a red line in these graphs. For the sample centrifuged at low angular acceleration (shown in Fig. 6d) the length l for the compressed sample remains within the error of the length calculated for the initial structure. This indicates that the initial low angular acceleration compression does not alter the surface area of the interface but simply modifies the shape. However, the sample centrifuged at higher angular acceleration (shown in Fig. 6e) does not show such agreement. The length appears to remain fairly similar at different heights within the cuvette but the length is approximately 10 μm lower than that for the initial structure. A reduced length corresponds to an increased interfacial area as a result of compression. This increase in the surface area might be due to the bulging of the sample towards the glass which occurs for this type of sample. This could mean that some of the interface is now supported by the glass walls allowing the particles to stabilise more surface area within the structure. These results combined with the confocal images suggest that particles are not being ripped off the interfaces at least at the angular accelerations investigated.[31–33]

3.3 Air bubbles

The scenario, outlined above, is modified in the majority of samples due to the presence of air bubbles (see Fig. 7a).

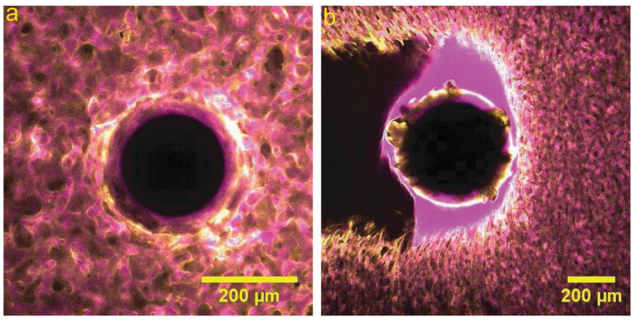

Fig. 7 (a) An image taken on the confocal microscope of an air bubble in a bijel with 5 vol% particles and an interface separation of 40 μm. (b) An image taken on the confocal microscope of a bubble in a bijel with 5 vol% particles and an interface separation of 23 μm after centrifuging for 5 minutes at 15*g* and the destruction of the structure it has caused. The ethanediol rich phase is coloured magenta and the particles are coloured yellow.

The first is air trapped within the silica particles and the second is nitrogen solubilised within the nitromethane which is released due to temperature changes as the sample is quenched. No air bubbles have been observed in bijels made from water, 2,6-lutidene and silica particles implying that the bubbles are more likely to originate from the temperature quench inducing a change in solubility of the nitrogen. The number of air bubbles observed in the bijels ranged from 0 to 200 but a majority of samples contained fewer than 20 bubbles.

Channels formed by the bubbles which reach the top of the compressed structure undermine the negative feedback response described in Section 3.2. This is the case because the air bubbles are significantly more buoyant than the surrounding structure and upon centrifugation, an enhancement of gravitational acceleration, these bubbles proceed upwards creating a path of destruction behind them (see Fig. 7b). If the angular acceleration and centrifugation time are high enough the bubbles can reach the top of the compressed bijel creating a large channel through the structure which ends at the top (see the inset in Fig. 8). The presence of these channels allows the liquids to depart the compressed bijel structure much more easily and hence leads initially to a larger macroscopic compression under centrifugation. Indeed, this effect can be observed in Fig. 8 where the initial permeability increases with increasing number of channels in the sample indicating that initial liquid movement is faster for samples which contain more channels. Since the initial permeability is also dependent on the domain size of the bijel the data have been grouped in this manner. This establishes that the withdrawal of the two liquids from the bijel structure is an essential aspect of the compression process. Channels caused by air bubbles such as the ones reported here have additionally been observed to aid settling in experiments on settling iron oxide suspensions.[34]

Although the solid particles provide the bijel with mechanical stability, we have found that the bijel is relatively easily deformed due in part to the density differences of the particles and liquids. We have demonstrated that it is possible to train the isotropic bijel structure into an anisotropic configuration

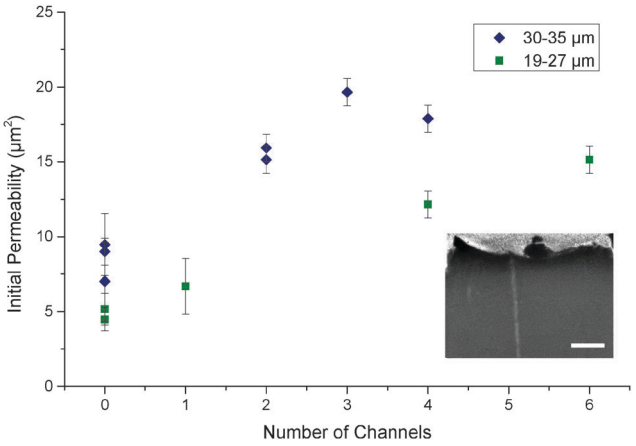

Fig. 8 A graph showing the relationship between the initial permeability and the number of channels caused by bubbles in the sample where blue diamonds are the bijels with a domain size of 30–35 μm and green squares are the bijels with a domain size of 19–27 μm. Inset: An image showing a channel in a sample after centrifugation. The scale bar is 2 mm.

with only modest stresses. This substantiates previous findings that liquid based templates for solid particles can be altered into new structures by centrifugal compression.[19] This style of experiment will allow us in the future to engineer out undesirable properties such as the presence of air bubbles within the structure. The information on the flow of liquids throughout the structure could be useful for applications involving liquid transport.

4 Conclusions

We have created bijels which have long term stability at 1*g* from nitromethane, ethanediol and silica particles and studied their response to centrifugal compression. As summarised below, we find that the response of the bijel is due to the combined roles of the permeability of the fluid channels and the unjamming and re-jamming of the interfaces.

At low angular accelerations, it takes many minutes for the bijel height to reach its final value. We find the permeability associated with bijel compression to be a consequence of the size of the domains through which the fluids flow. Higher permeabilities are found in bijel samples that contain air bubbles, which rise to the surface during compression and provide routes for fluids to escape. Hence, these samples are initially compressed faster.

Microscopically, the bijel undergoes internal distortion under compression. At lower angular accelerations, internal yielding is observed: below some height in the sample the bijel structure becomes anisotropic. The initially sponge-like arrangement of domains comes to resemble sheets aligned perpendicular to the compression direction. In this regime the interfacial area that is stabilised remains constant along the height of the sample. At higher angular accelerations the entire structure appears to buckle on a longer length scale – apparently associated with occupying a wetting layer close to the vial wall. After centrifugation has ceased, the interfaces appear to have re-jammed in all cases and the bijel shows no macroscopic elastic recovery. The latter is because the less dense fluid is blocked from re-entering the bicontinuous structure.

The microscopic and permeability characteristics combine to give the bijel a negative feedback response to compression: the microscopic rearrangements serve to make it more difficult for the fluids to escape. This implies that the permeability decreases as compression proceeds.

Acknowledgements

K. A. R. thanks EPSRC for PhD, studentship funding with the Condensed Matter Doctoral Training Centre (CM-CDT) under grant number EP/G03673X/1. J. H. J. T. acknowledges the Royal Society Research Grant, Royal Society of Edinburgh/BP Trust Research Fellowship and The University of Edinburgh for a Chancellor's Fellowship for funding. We also thank EPSRC for funding under grant number EP/J007404/1 and M. Reeves for assistance with calculating interfacial separations.

References

1 E. M. Herzig, K. A. White, A. B. Schofield, W. C. K. Poon and P. S. Clegg, *Nat. Mater.*, 2007, **6**, 966–971.
2 K. Stratford, R. Adhikari, I. Pagonabarraga, J.-C. Desplat and M. E. Cates, *Science*, 2005, **309**, 2198–2201.
3 B. P. Binks and T. S. Horozov, *Colloidal Particles at Liquid Interfaces*, Cambridge University Press, New York, 2008.
4 J. W. Tavacoli, J. H. J. Thijssen, A. B. Schofield and P. S. Clegg, *Adv. Funct. Mater.*, 2011, **21**, 2020–2027.
5 J. A. Witt, D. R. Mumm and A. Mohraz, *Soft Matter*, 2013, **9**, 6773–6780.
6 M. N. Lee, J. H. J. Thijssen, J. A. Witt, P. S. Clegg and A. Mohraz, *Adv. Funct. Mater.*, 2013, **23**, 417–423.
7 M. E. Cates and P. S. Clegg, *Soft Matter*, 2008, **4**, 2132–2138.
8 M. N. Lee and A. Mohraz, *Adv. Mater.*, 2010, **22**, 4836–4841.
9 M. N. Lee, M. A. Santiago-Cordoba, C. E. Hamilton, N. K. Subbaiyan, J. G. Duque and K. A. D. Obrey, *J. Phys. Chem. Lett.*, 2014, **5**, 809–812.
10 J. A. Witt, D. R. Mumm and A. Mohraz, *J. Mater. Chem. A*, 2016, **4**, 1000–1007.
11 M. Cui, T. Emrick and T. P. Russell, *Science*, 2013, **342**, 460–463.
12 D. Cai and P. S. Clegg, *Chem. Comm.*, 2015, **51**, 16984–16987.
13 M. F. Haase, K. J. Stebe and D. Lee, *Adv. Mater.*, 2015, **27**, 7065–7071.
14 H. Firoozmand and D. Rousseau, *Food Hydrocolloids*, 2015, **48**, 208–212.
15 L. Bai, J. W. Fruehwirth, X. Cheng and C. W. Macosko, *Soft Matter*, 2015, **11**, 5282–5293.
16 M. Reeves, A. T. Brown, A. B. Schofield, M. E. Cates and J. H. J. Thijssen, *Phys. Rev. E*, 2015, **92**, 032308.
17 M. Reeves, K. Stratford and J. H. J. Thijssen, *Soft Matter*, 2016, DOI: 10.1039/c5sm03102h.

18 K. N. Nordstrom, E. Verneuil, W. G. Ellenbroek, T. C. Lubensky, J. P. Gollub and D. J. Durian, *Phys. Rev. E*, 2010, **82**, 041403.
19 L. Maurice, R. A. Maguire, A. B. Schofield, M. E. Cates, P. S. Clegg and J. H. J. Thijssen, *Soft Matter*, 2013, **9**, 7757–7765.
20 S. Arditty, V. Schmitt, F. Lequeux and F. Leal-Calderon, *Eur. Phys. J. B*, 2005, **44**, 381–393.
21 E. Kim, K. Stratford and M. E. Cates, *Langmuir*, 2010, **26**, 7928–7936.
22 P. C. Millett, *J. Chem. Phys.*, 2014, **140**, 144903.
23 K. A. White, A. B. Schofield, P. Wormald, J. W. Tavacoli, B. P. Binks and P. S. Clegg, *J. Colloid Interface Sci.*, 2011, **359**, 126–135.
24 J. Y. Huh, M. L. Lynch and E. M. Furst, *Phys. Rev. E*, 2007, **76**, 051409.
25 R. Buscall and L. R. White, *J. Chem. Soc., Faraday Trans.*, 1987, **83**, 873–891.
26 F. A. L. Dullien, *Porous Media: Fluid Transport and Pore Structure*, Academic Press, 1992.
27 S. Manley, J. M. Skotheim, L. Mahadevan and D. A. Weitz, *Phys. Rev. Lett.*, 2005, **94**, 218302.
28 C. Rotella, S. Tence-Girault, M. Cloitre and L. Leibler, *Macromolecules*, 2014, **47**, 4805–4812.
29 H. Tanaka and T. Araki, *Europhys. Lett.*, 2000, **51**, 154–160.
30 L. Starrs, W. C. K. Poon, D. J. Hibberd and M. M. Robins, *J. Phys.: Condens. Matter*, 2002, **14**, 2485–2505.
31 J. W. Tavacoli, G. Katgert, E. G. Kim, M. E. Cates and P. S. Clegg, *Phys. Rev. Lett.*, 2012, **108**, 268306.
32 M. Abkarian, S. Protière, J. M. Aristoff and H. A. Stone, *Nat. Commun.*, 2013, **4**, 1895.
33 D. Vella, *Annu. Rev. Fluid Mech.*, 2015, **47**, 115–135.
34 G. G. Glasrud, R. C. Navarrete, L. E. Scriven and C. W. Macosko, *AIChE J.*, 1993, **39**, 560–568.